Composites Part A: Applied Science and Manufacturing
January 2022, Volume 152 Issue Part A Pages 106719 (10p.)
https://doi.org/10.1016/j.compositesa.2021.106719
https://archimer.ifremer.fr/doc/00735/84662/

Archimer
https://archimer.ifremer.fr

A study of pure hydrolysis of carbon fibre reinforced polyamide 6 composites tested under mode I loading

Arhant Mael [1, *], Lolive Eric [2], Bonnemains Thomas [2], Davies Peter [1]

[1] IFREMER, Marine Structures Laboratory, Centre de Bretagne, Plouzané, France
[2] IUT de Brest, IRDL, Brest, France

* Corresponding author : Mael Arhant, email address : mael.arhant@ifremer.fr

eric.lolive@univ-brest.fr ; thomas.bonnemains@univ-brest.fr ; peter.davies@ifremer.fr

Abstract :

This paper focuses on the durability of carbon/polyamide 6 thermoplastic composites subjected to hydrolytic aging and tested under mode I static crack growth loading. In this study, aging was performed at temperatures ranging from 100 to 140 °C for durations up to 3 months in oxygen-free water. Results show that following wet aging the fracture toughness (energy release rate) decreases significantly, from an unaged value of 3.4 kJ/m2 down to values below 1 kJ/m2 after extensive degradation. This decrease was associated with a change from ductile to brittle behaviour, which allowed a critical molar mass M'c, to be determined for the first time on long carbon fibre reinforced composites.

Highlights

► A critical molar mass was identified for the first time on a long carbon fibre reinforced composite. ► Even after extensive ageing degradation, the fracture toughness of C/PA6 composite is similar to those of unaged C/Epoxy composites. ► It is possible to predict the long term fracture behaviour of C/PA6 using an Arrhenius approach.

Keywords : Thermoplastic composites, Mode I fracture, Hydrolysis, Molar mass, Arrhenius

Please note that this is an author-produced PDF of an article accepted for publication following peer review. The definitive publisher-authenticated version is available on the publisher Web site.

1. Introduction

Due to their excellent specific properties, composite materials have replaced a significant number of structural metallic components. They are now found in almost every industrial application, from automotive to aviation but also in the marine industry (tidal turbines, pleasure boats, military vessels, offshore applications, etc.). Most industrial composite materials are based on carbon and glass fibres coupled with either polyester or epoxy matrix, i.e. thermoset resins. However, such materials often show poor impact resistance mostly induced by a low fracture toughness [1]. Ways to increase that particular property include adding fillers to the thermoset matrix, such as sand, rubber or thermoplastic particles [2], or to directly work with a thermoplastic matrix. The latter is particularly interesting because most thermoplastics exhibit mode I fracture toughness values above 1 kJ/m² while thermosets usually show values below 1 kJ/m² [3]. However, for marine applications it is essential to investigate whether such thermoplastics retain their high fracture toughness after long term exposure to sea water. The

durability of thermoset composites in the marine environment has been the subject of a large number of papers over the past 40 years [4, 5, 6, 7]. Depending on the degradation mechanism, the fracture toughness evolves in different ways. Short term exposure to water usually leads to an increase in the fracture toughness induced by the plasticization of the matrix while long term exposure (oxidation, hydrolysis, fibre/matrix debonding) leads to a decrease in fracture toughness [8, 9]. Despite having high initial fracture toughnesses, the durability of thermoplastic composites has not received the same attention, and fewer fracture test results are available in the literatures. However, other aspects of the durability of thermoplastic composites in a marine environment have been studied extensively, as demonstrated by the publication of guidelines by the Offshore Oil and Gas industry [10,11] and published results [12, 13]. These mostly show that materials such as C/PEEK keep their excellent properties in sea water, even after long periods of immersion at high temperature [12], provided that the fibre/matrix interface is not degraded upon aging [14]. Other material systems have also been investigated, from polyamides to acrylic matrices [15, 16]. Concerning fracture tests specifically, back in 1992, Hoa et al. [17] investigated the influence of hygrothermal aging on the mode II fracture toughness of C/PPS laminates. An increase in the fracture toughness was observed as the water content within the specimens increased. The latter was associated with plasticization of the matrix. This was also observed on Glass/polypropylene specimens immersed in water for 5 months by Davies et al. in 1995 [18]. Also in 1995, Seltzer and Friedrich [14] studied the mode II fracture toughness of C/PEEK composites before and after water saturation. They showed a decrease from 3.90 kJ/m² down to 3.13 kJ/m² after saturation. This was explained by fibre/matrix debonding, highlighted by SEM fracture surfaces. A few years later, Zenasni et al. [19] studied the fracture behaviour of glass and carbon/PEI laminates after aging at 70°C and 95% humidity. In mode I, the fracture properties were decreased by 10 % after two months of aging. Very few other papers were found in literature concerning the crack growth behaviour of thermoplastic composites subjected to hygrothermal aging.

To investigate the phenomena that are linked with a decrease in fracture toughness in more detail, it is of particular interest to take a look at the work of the polymer degradation community where a large number of papers on the aging behaviour of thermoplastics have been published. In particular, it has been highlighted several times that when investigating degradation processes such as oxidation and hydrolysis, i.e. irreversible phenomena that may occur upon sea water aging, the molar masses, in number (M_n) or in weight (M_w), are interesting markers to follow aging [20-22]. Indeed, upon oxidative or hydrolytic aging, the molar mass decreases and can be linked with mechanical properties [23, 24]. Some authors have directly linked the loss in polymer fracture toughness upon aging with the molar mass [25, 26]. However, very few studies used such a marker when working on the durability

of long fibre reinforced thermoplastic composites. Recently, Le Gac and Fayolle [27] investigated the tensile behaviour of short glass fibre reinforced polyamide 6.6 composites after hydrolytic aging. However, no fracture tests were performed. In 2004, Pegoretti and Penati [28] used fracture tests to study the effect of hygrothermal aging on short glass fibre reinforced recycled PET composites. However, to the knowledge of the authors, no studies linking the molar mass to the mode I fracture properties have been performed on long fibre reinforced composites. This is one of the two aims of the present study. The second is to be able to predict the loss in mode I fracture toughness after hydrolytic aging.

First, the material and techniques used in this paper will be presented. Second, the effect of hydrolytic aging is investigated at one aging temperature, 120°C, in order to assess the changes both in terms of mode I fracture toughness and microstructure (molar mass, crystallinity ratio, etc.). Then, results will be presented at other aging temperatures, in order to try to generalize the changes in behaviour. Finally, results from fracture toughness tests after aging will be linked with the molar mass and will be used to translate the results from accelerated aging to service temperature through an Arrhenius approach.

2. Materials and Methods

2.1. Materials

The carbon/polyamide 6 material used in this work was supplied by Celanese (Reference: CFR-TP-PA6-CF60-01) in the form of a 125 µm thick unidirectional prepreg sheets. From these, unidirectional carbon/polyamide 6 panels (dimensions 280 x 280 x 5 mm^3) were manufactured by press forming on a DK Technologies press (40 plies total) at a temperature of 240°C and a pressure of 5 bars. The cooling rate was about 20°C/min. It may be noted that these manufacturing parameters differ from those recommended by the manufacturer and more especially a suggested temperature of 271°C. Using that temperature of 271°C, we were not able to obtain flat panels as a significant amount of matrix flowed out of the mold and induced fibre misalignments within the panel. A PTFE insert (dimensions 280 x 80 x 0.025 mm^3) was located at mid-thickness on one end of each panel. Double Cantilever Beam (DCB) specimens with dimensions 250 x 20 x 5 mm^3 were then produced using a water jet cutting machine. A fibre volume fraction of 48% was obtained along with a crystallinity ratio of 38% and an initial molar mass of 26.2 kg/mol.

2.2. Double cantilever beam (DCB) tests

Mode I fracture tests were performed on an Instron testing machine (5561) using a load cell of 500 N at a test speed of 1 mm/min. To record the crack length along the test, a Basler camera was used at a frame rate of 1

picture per second. Instead of aluminium tabs, glass/polyamide 6 tabs were used here to ensure a better interface with the specimens. Tabs dimensions were (20 x 20 x 10 mm^3). For each condition, three repeat specimens were used and all specimens were dried in desiccators at 0% humidity before testing. Tests were performed according to ASTM 5528 [29] using the compliance calibration method (CC), Eq.1.

$$G_{IC} = \frac{nP\delta}{2ba} \quad \text{Eq.1}$$

Where P is the applied load, δ the displacement. b and a are respectively the width and the thickness of the DCB specimen and n is the slope of the log δ/P versus log a plot. All specimens were pre-cracked a few millimetres under mode I loading before test, as the PTFE starter film insert was thicker than that specified by the standard, so only propagation results are shown in this paper.

2.3. Aging

DCB specimens and small coupons (50 x 50 mm^2) for physicochemical characterization were immersed in deionised water at temperatures ranging from 100 up to 140°C °C within small pressure vessels. A pressure of 15 bar was applied to ensure liquid water upon aging. Different aging durations were chosen, ranging from 1 day up to 90 days. To ensure that hydrolysis is the only degradation phenomenon taking place, the oxygen contained within the deionised water was removed by nitrogen saturation. For each aging condition, the nitrogen saturation process lasted for three hours until all the oxygen had been removed. This was checked with an oxygen sensor. Such high aging temperatures were chosen based on the work of Deshoulles et al. [30] who recently studied the effect of pure hydrolysis on neat PA6. They highlighted that such a process is very slow. Indeed, upon aging at 80°C, the PA6 loses less than 2% of its initial mass after 500 days of aging. Also, using the Arrhenius law, they predicted that it would take more than 1000 years at 25°C for the material to lose 1 % of its initial mass.

This water absorption in Polyamide 6 significantly decreases the glass transition from 66°C in the dry state down to -12°C at a water content of about 10% within the matrix [16]. Such a significant loss in glass transition is not usually observed (typically, the loss in glass transition temperature of an epoxy after water saturation is about 20°C). This significant decrease in glass transition implies that upon aging in water in real conditions (between 4 to 30°C), polyamide 6 will eventually turn into the rubbery state because of the negative T_g. Once in the rubbery state, the polyamide 6 polymer no longer faces changes in state up until the crystallization temperature (around 160°C). After water saturation, the polymer therefore remains in the same state (rubbery) at 25°C and at 140°C.

After each aging condition, all the specimens were dried in desiccators at 0% humidity until stable weight was reached. Initially, it was intended to test the specimens both in the dry state and also right after aging, i.e. in

the fully saturated state. However, DCB tests performed on fully saturated specimens did not allow any crack propagation, as the upper DCB arm systematically failed in flexure on the compression side due to the loss in properties induced by water ingress.

2.4. Weight measurements

Weight measurements were performed to follow the mass changes that occur upon aging. To do so, the specimens were weighed before aging in the dry state (m_0), straight after aging in water (m_{sat}) and also after a second drying process (m_d). The three measurements allow for the definition of three different quantities. First, the traditional one which defines the change in weight from the initial state m_0 to the one after aging m_f, here called mass changes, Eq. 1:

$$Mass\ changes = \frac{m_{sat} - m_0}{m_0} \quad \text{Eq. 1}$$

Usually, the quantity defined in Eq. 1 is associated with water content. However, in our case, hydrolysis leads to a leaching of macromolecular chains in the water, which induces a mass loss. So the water content is actually determined from Eq. 2 and the mass loss from Eq. 3:

$$Water\ content = \frac{m_{sat} - m_d}{m_d} \quad \text{Eq. 2}$$

$$Mass\ loss = \frac{m_d - m_0}{m_0} \quad \text{Eq. 3}$$

2.5. Differential Scanning Calorimetry (DSC)

Degrees of crystallinity X_c were determined using DSC on Q200 equipment from TA instruments at a heating rate of 10°C/min from ambient temperature to 300°C. In composite materials, the degree of crystallinity X_c is determined as follows, Eq. 4:

$$X_c = \frac{\Delta H_f}{\Delta H_f^0 \times (1 - W_f)} \quad \text{Eq.4}$$

Where ΔH_f is the enthalpy of fusion of the tested polymer, ΔH_f^0 the theoretical enthalpy of fusion for a 100% crystalline material, taken equal to 118 J/g [31] and W_f the fibre weight fraction. The latter was determined by TGA from matrix burn off tests at 450°C for 2 hours under nitrogen (N_2).

2.6. Size Exclusion Chromatography (SEC)

Molar mass was determined by SEC by the PeakExpert Company according to the Laun and al. method [32]. These tests allow for the determination of the average molar mass in number (M_n) and in weight (M_w) but also the polydispersity index (PDI). To obtain these values, samples of 10 mg were dissolved in 4 mL of hexafluoroisopropanol (HFiP). The detection was performed using a Waters 2414 differential refractive index detector and data were analysed with PSS WinGPC unity v7.5 SEC software. The calibration was performed using poly(methyl methacrylate) standards supplied by PSS GmbH Mainz, Germany, with molar mass ranging between 800 and 1,600,000 g/mol and the calibration curve was adjusted with a 5th order polynomial. Calculations are conventional and average molecular weights are expressed as PMMA equivalents.

2.7. Quality control

2.7.1. Scanning electron microscopy (SEM)

SEM microscopy was used to characterize the microstructure of the composite immediately after aging. To do so, specimens were embedded in epoxy resin and then polished gradually from 320µm down to 1µm abrasive papers. SEM was also used to observe the fracture surfaces after failure. In both cases, the aim was to investigate whether aging has an effect on the microstructure and fracture surfaces.

2.7.2. X-Ray Tomography

X-Ray tomography was performed on a high-resolution GE/Phoenix tomograph by the CRT located in Morlaix. It was used to observe the changes in macrostructure across the cross sections after different aging durations. The VG Studio software was used for the data treatment.

3. Results

Results are first presented at one specific temperature (120°C). This allows us to describe the consequences induced by aging at this specific temperature. Second, results are generalized to all the aging temperatures considered in this study.

3.1. Aging performed at 120°C

3.1.1 Weight changes

Water ingress can have a significant effect on the mechanical properties of polyamide 6 based composites [16]. Here, the water content was characterised by weighing the specimens after different aging times. These same specimens were also dried in desiccators until stable weight was reached in order to obtain the mass loss induced by aging. Results are presented in Figure 1 for aging durations up to 28 days at 120°C and show that the water

content increases significantly at the very beginning of the aging process (from 0 to 1 day of aging) and then increases gradually up to 5.8% after 28 days of aging. On the other hand, the mass loss evolves throughout the aging process. After 28 days of aging, the specimens lost around 1.5% of their initial mass. Knowing that carbon fibres are insensitive both to a temperature of 120°C and to water, this suggests that the mass loss is associated with an irreversible degradation of the matrix and therefore a loss of about 3.8 % within the matrix itself.

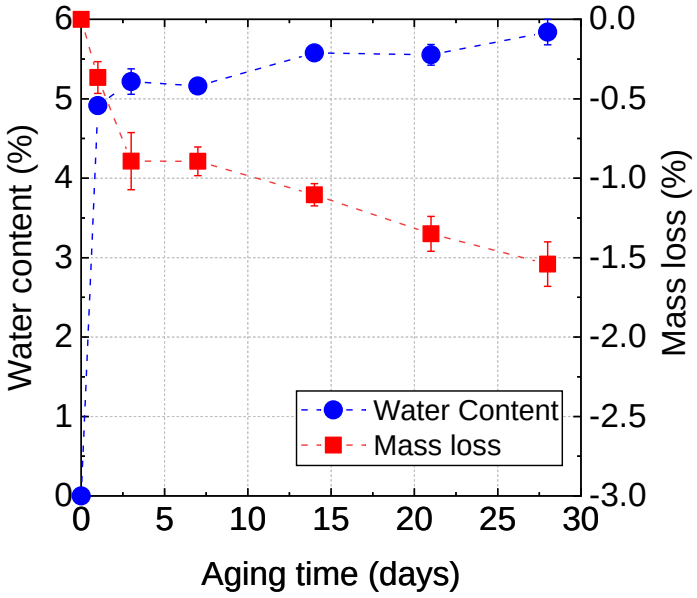

Figure 1: Effect of aging on water content during aging and mass loss after water desorption

Also, to a first approximation, using the data from published work by the authors [33] ($D=5.08.10^{-14}$ m²/s and $M_{sat}=3.23\%$) and assuming a Fickian diffusion (not exactly the case in PA6, see [34]), we can approximate a time to saturation at 15°C on a 5 mm thick specimen of about 3 years while at 120°C, the water saturation is reached within a day. This clearly demonstrates the acceleration provided by aging at 120°C.

3.1.2. Physico-chemical modifications

This section is devoted to the effect of aging on the physico-chemical properties of carbon/polyamide 6 DCB specimens. First, molar mass results are presented in Figure 2.a and Figure 2.b. It is observed on Figure 2.a that as the aging duration increases the curves tend to shift towards higher elution volume values, which indicates a decrease in the molar mass. Also, the shape of each curve does not change with aging, which suggest a constant polydispersity index upon aging. This confirms that a statistical chain scission process happens upon hydrolysis. Results from Figure 2.a are confirmed on Figure 2.b, i.e., the molar mass decreases rapidly from 26 kg/mol until

it reaches 11 kg/mol after 28 days of aging and the polydispersity index does not evolve during aging (around 2.3). This is directly associated with the hydrolysis of the amorphous phase in the polyamide 6 matrix. The mass loss observed in Figure 1 may be associated with the migration of small molecular weight chains in water during aging, as suggested by Verdu [35].

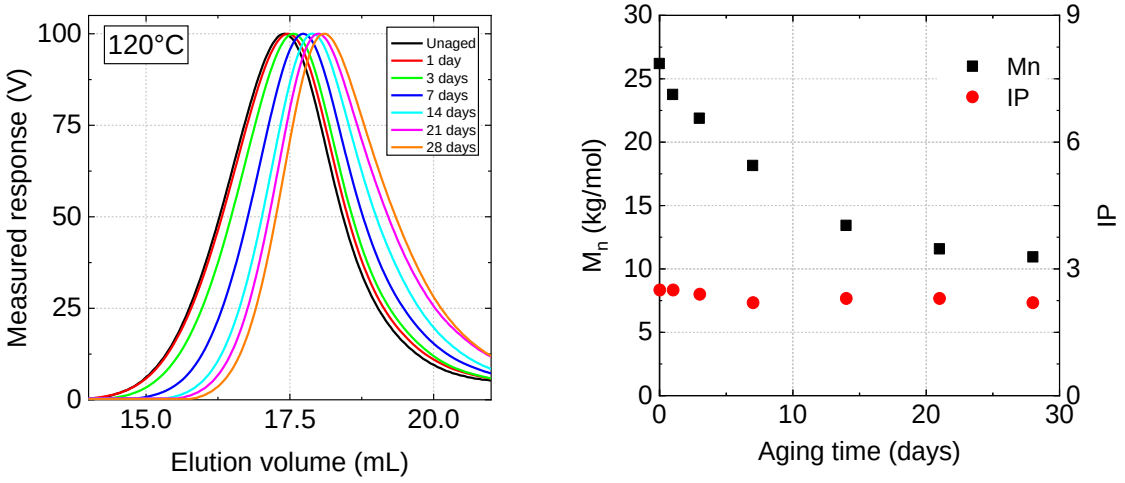

(a) (b)

Figure 2: Effect of aging at 120°C on (a) Response from SEC measurements and (b) Molar mass and polydispersity index

Together with a decrease in the molar mass, an increase in the crystallinity ratio is observed during aging as shown in Figure 3. First, Figure 3.a shows the change in melting peak for different aging durations. Results show that as the aging time increases, we see an increase in the enthalpy of the melting peak. Also, there is no change in the form of the melting peak. Then, on Figure 3.b, we see that after 28 days of aging, the crystallinity ratio increases from 38% up to 49%. This process is associated with the chemi-crystallization phenomenon, well known in the literature [36]. As chain scission occurs, the amorphous chains within the polymer regain enough mobility to form new crystallites. Also, it is believed that upon aging, the fibres do not play a major role on the chemi-crystallization process. It is known that upon cooling from the melt, fibres play a significant role as they initiate preferential nucleation sites close to the fibres. However, here, the matrix is in the solid-state during aging and does not go into the melted state. Additionally, the increase in crystallinity ratio seen here is of the same order of magnitude as the increase observed on neat PA6 in [30].

Both of these changes (decrease in molar mass and increase in crystallinity ratio) are expected to have a significant effect on the crack growth properties in the composite. However, these changes are associated with the

polyamide 6 matrix only, while the material of interest here is a composite material. Therefore, modifications in the structure of the composite are also expected.

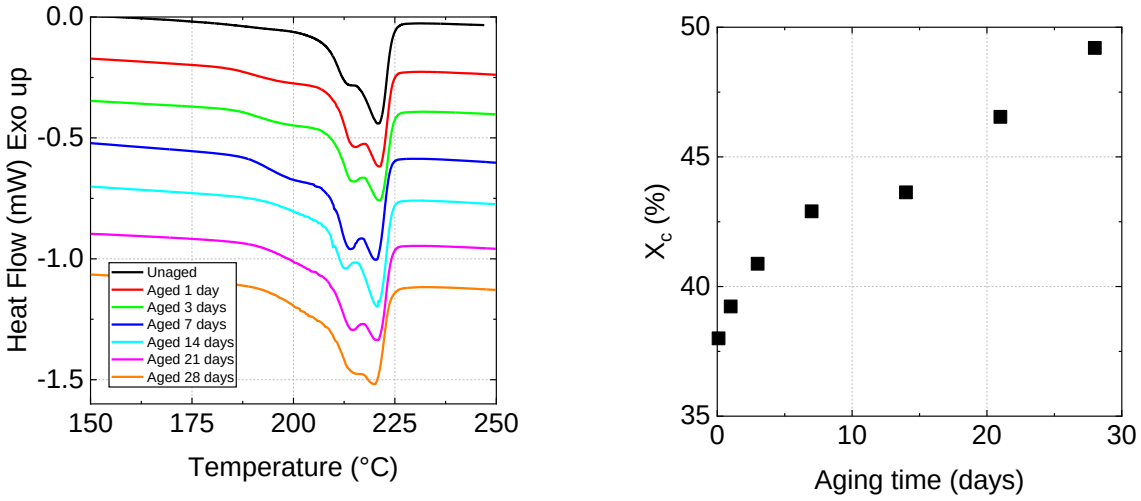

(a) (b)

Figure 3: Effect of aging at 120 °C on (a) the melting peak (b) the crystallinity ratio

3.2. 3.1. Changes in specimen microstructure

Changes in composite structure were first investigated using X-ray Tomography, in order to observe the macrostructure at the specimen scale, Figure 4.

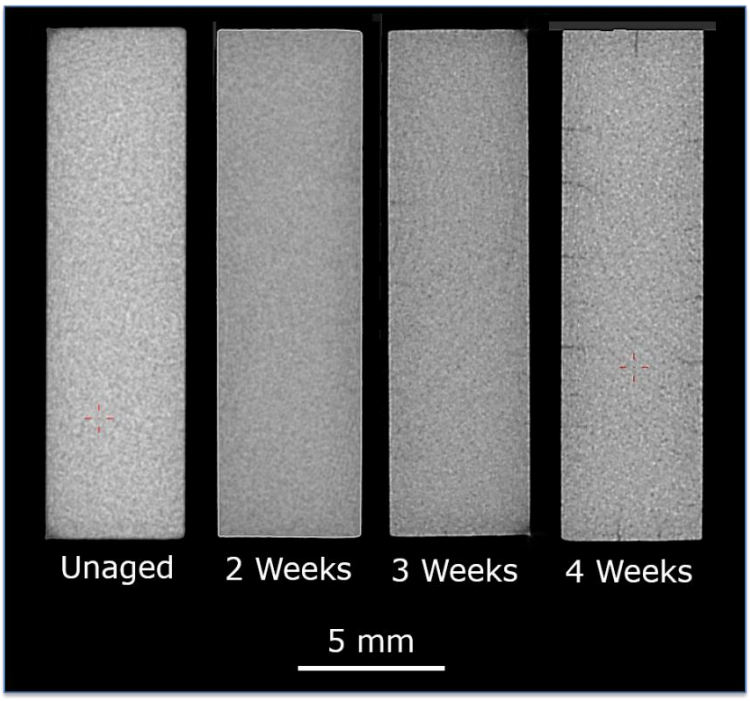

Figure 4: Specimen cross sections observed using X-ray tomography after different aging durations

The X-ray scans presented in Figure 4 show that as aging duration increases, macroscopic transverse cracks start to appear after 14 days of aging while no cracks are observed before. Most of these cracks are 1 mm long, which is significant. It may be noted that this does not mean that transverse cracks do not exist before 14 days of aging. Here, the voxel size is limited to 36µm, i.e. much higher than the fibre scale. Therefore, to examine this in more detail SEM microscopy was used to observe the microstructure at the fibre and matrix scale, Figure 5.

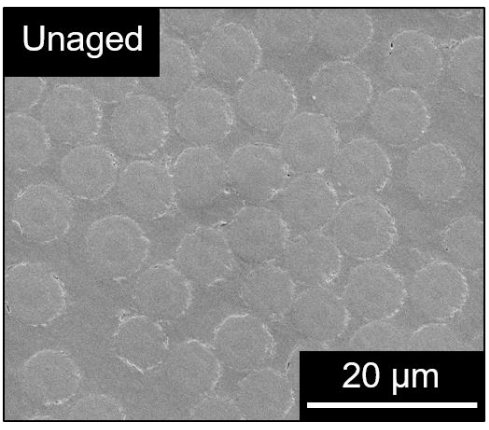

(a)

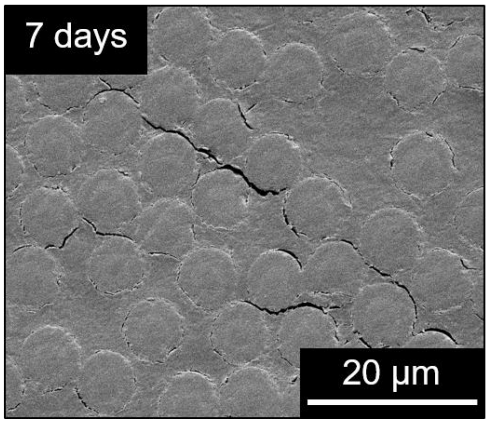

(b)

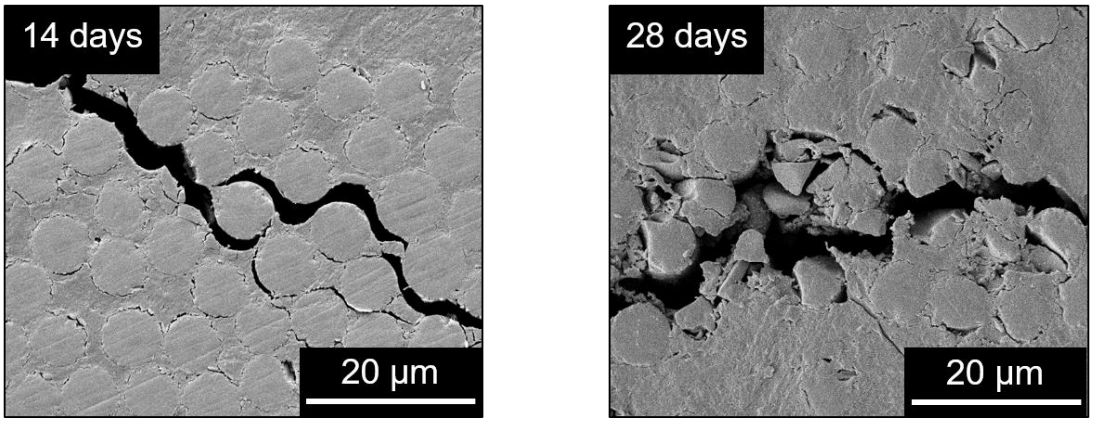

(c) (d)

Figure 5: SEM micrographs observed after different aging durations (a) Unaged (b) Aged 7 days (c) Aged 14 days (d) Aged 28 days

SEM micrographs presented in Figure 5 provide additional information compared with Figure 4 as they show that the transverse cracks are located close to the fibre/matrix interface. No cracks are observed in the unaged state but cracks are visible after 7 days of aging, which were not observed using X-ray tomography. Also, as aging time increases, cracks extend. Additionally, Figure 5.d suggests that carbon fibres seem to be affected by aging. However, the authors believe that this visible degradation is not due to the aging process but rather the polishing stage on a highly degraded material.

All these physico-chemical and microstructural changes suggest that aging will also have an effect on the fracture toughness properties of carbon/polyamide 6 composites.

3.3. Effect of aging on the fracture toughness properties

Results from DCB tests on specimens tested in the unaged state and after several aging durations are shown in Figure 6.a. Then, associated fracture toughness values are shown in Figure 6.b.

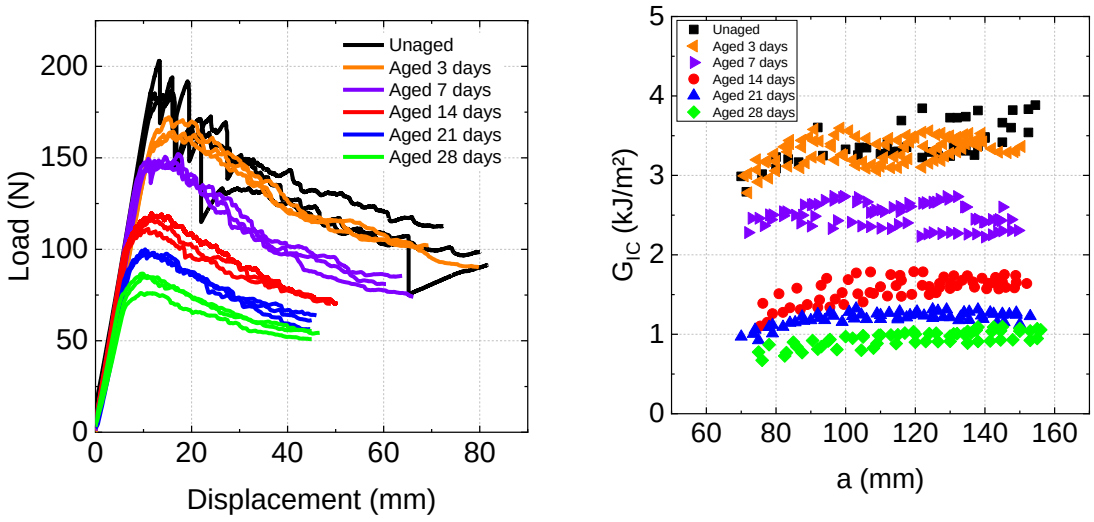

(a) (b)

Figure 6: Effect of aging on (a) Load-displacement plots (b) Fracture toughness R-curves

Results from Figure 6.a show that aging has a significant effect on the load-displacement plots. Concerning unaged specimens, crack growth propagation starts around 170N while after 28 days of aging, propagation starts around 80N. As a consequence, the associated fracture toughness values are greatly diminished as a function of aging, Figure 6.b. Initial unaged values are above 3kJ/m² in the unaged state while values after aging drop below 1 kJ/m². To present the fracture toughness values more clearly, mean values are plotted as a function of aging time in Figure 7.

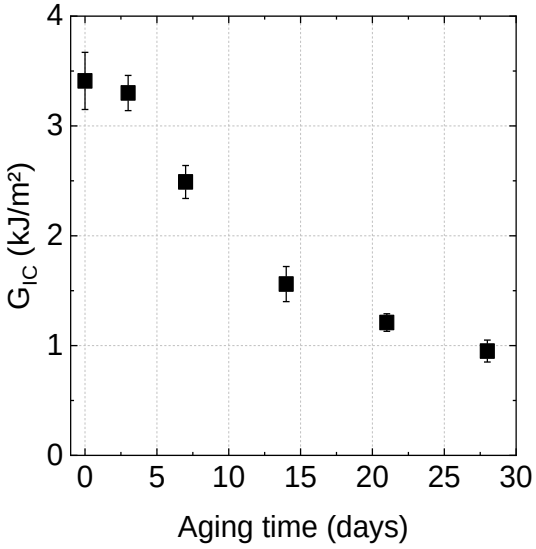

Figure 7: Fracture toughness versus aging time

From Figure 7, fracture toughness decreases from 3.44 ± 0.28 kJ/m² in the unaged state down to 0.94 ± 0.10 kJ/m² after 28 days of aging, so a factor of 3 reduction. Such a decrease suggests a clear change in mechanical behaviour. To support this, fracture surfaces before and after aging are shown in Figure 8.

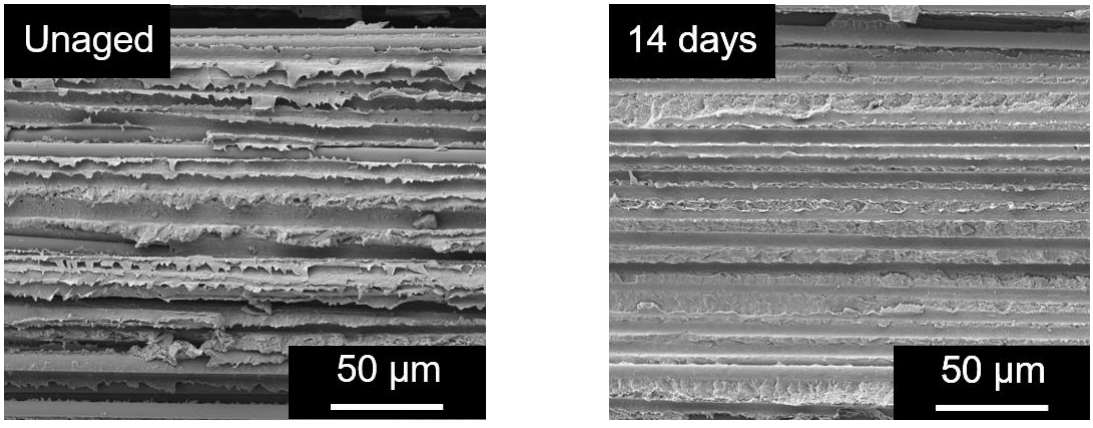

(a) (b)

Figure 8: Fracture surfaces (a) before aging (b) after aging

In Figure 8.a, failure surfaces show plastic deformation of the matrix in the unaged state while after aging a ductile/brittle transition is observed, Figure 8.b. Therefore, it may be noted that the decrease in fracture toughness observed here is very significant. Nonetheless, even after 28 days of aging the residual fracture toughness values lie in the same range as those of many carbon/epoxy composites [3].

3.2. Effect of aging temperature

The aim of this section is to investigate whether the different consequences observed after aging at 120°C are common for other temperatures, i.e. whether temperature only works as an accelerating aging factor. To do so, C/PA6 DCB specimens were aged in water at three other temperatures (100, 130 and 140°C) for different durations. First, results concerning the changes observed on the mass loss, molar mass and crystallinity ratio are shown in Figure 9.a, Figure 9.b and Figure 9.c, respectively.

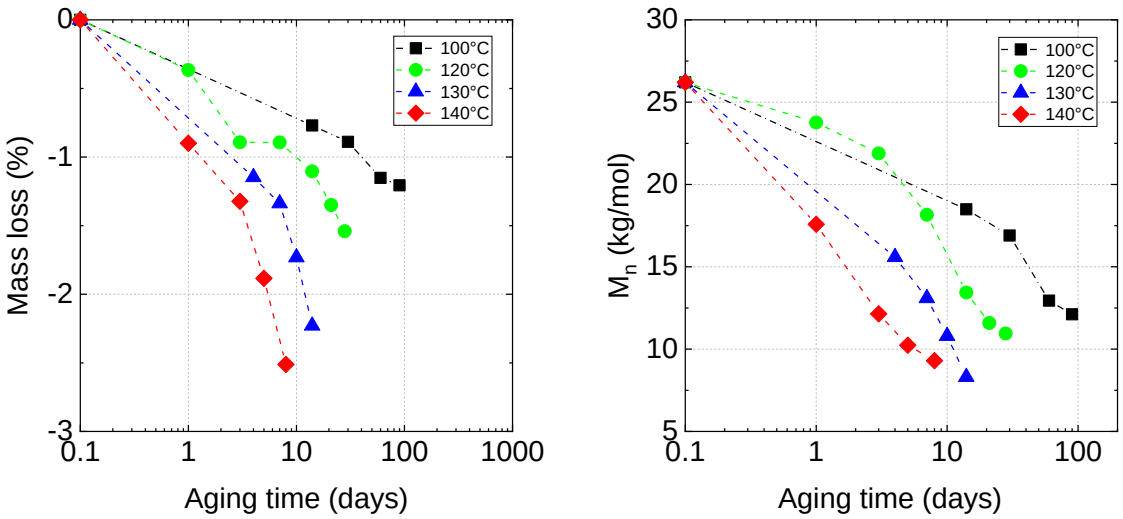

(a) (b)

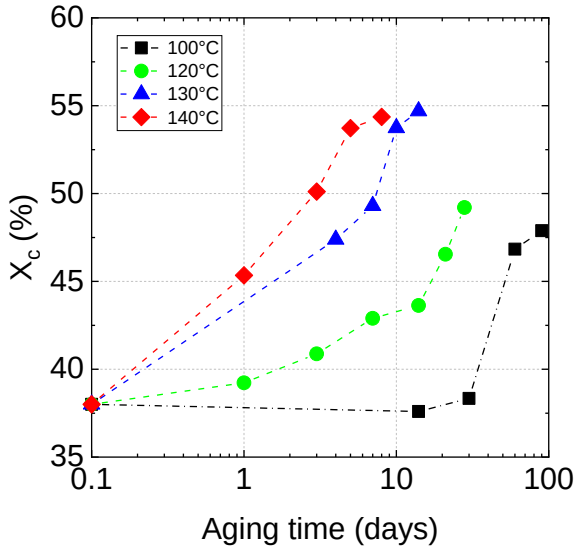

(c)

Figure 9: Effect of aging temperature on (a) Mass loss (b) Molar mass (c) Crystallinity ratio

These results show that the higher the temperature, the faster the change in mass loss, molar mass drop, and crystallinity ratio increase. Also, whatever the aging temperature, the same behaviour is observed; a decrease in the mass loss and molar mass and an increase in the crystallinity ratio. This suggests that temperature only plays an accelerating role here.

The effect of aging temperature on fracture toughness was then investigated. R-curves from DCB tests performed after aging at different temperatures are presented in Figure 10. For the three temperatures, a common behaviour is observed where the R curve is strongly affected by aging, in a similar way to that observed for an aging temperature of 120°C (Figure 6).

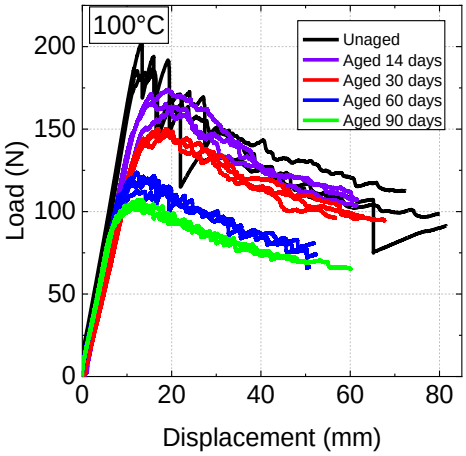

(a)

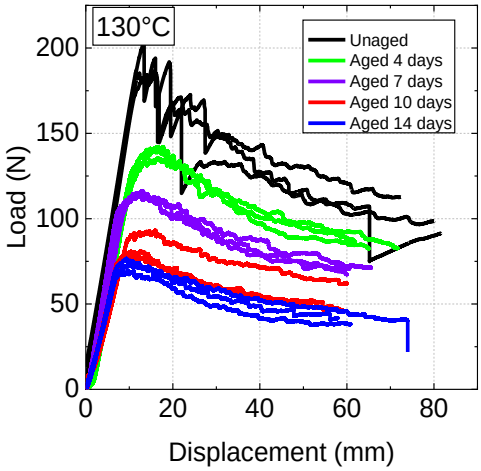

(b)

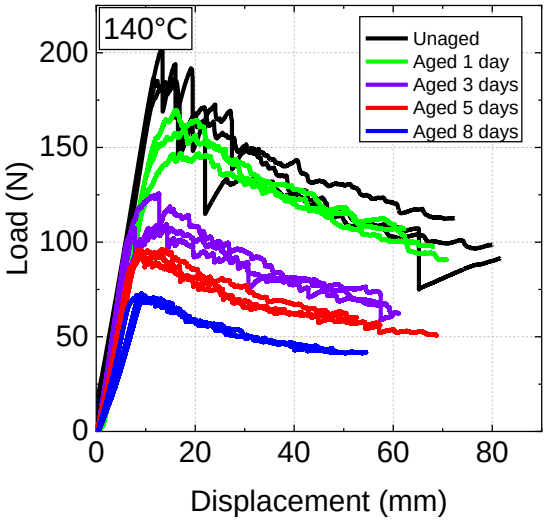

(c)

Figure 10: Effect of aging temperature on DCB curves (a) 100°C (b) 130°C (d) 140°C

Results showing fracture toughness as a function of time and for the different aging temperatures are shown in Figure 11. These show that at early aging durations, the fracture toughness seems to remain constant until a critical time where a significant decrease is observed. Also, linear elastic behavior is assumed in the calculation of G used in this test method. As noted in the standard mode I test protocol [29] this assumption is only valid when the zone of damage or nonlinear deformation at the delamination front, is small relative to the smallest specimen dimension. The load-displacement plots show a linear response up to crack initiation in all cases, suggesting that the damage zone is confined to the crack tip. Also, no permanent DCB arm deformation was noted

on unloading, and the crack remained at the specimen mid-plane throughout. For these reasons we believe that the use of the LEFM analysis is appropriate here.

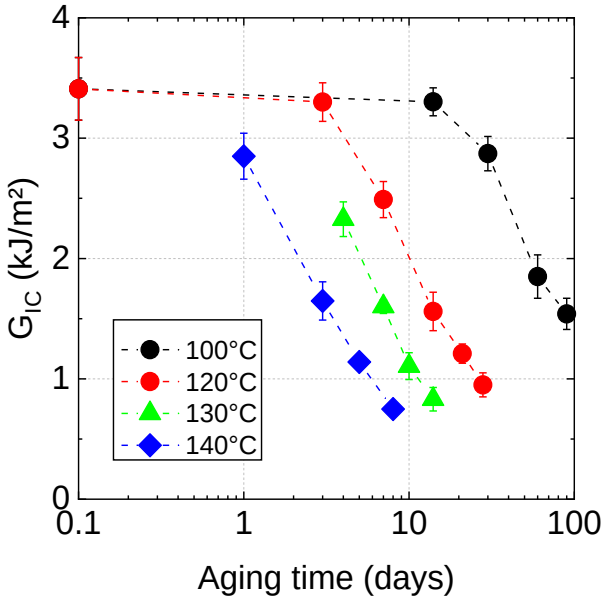

Figure 11: Effect of aging temperature on fracture toughness

Similarly to the results presented in section 3.1 after aging at 120°C, comparable tendencies are observed when performing aging at different temperatures (100°C, 130°C and 140°C). To sum up, whatever the aging temperature, hydrolysis of C/PA6 induces:

- A decrease in the molar mass
- An increase of the crystallinity ratio
- An increase in the mass loss
- A decrease in the fracture toughness

4. Discussion

Based on the results presented in the previous section, two main questions can now be addressed. First, it has been shown in the literature that fracture toughness can be linked with the molar mass for neat polymers. It is interesting to assess whether this is also confirmed on continuous fibre reinforced composites. Second, it is of particular interest to investigate whether the results can be described by an Arrhenius law, in order to propose a prediction at ambient temperatures.

4.1. Correlation between fracture toughness and molar mass – Identification of a critical molar mass

It has been shown many times in the literature that the fracture toughness can be directly linked with the molar mass of several neat polymers [26, 28, 37]. Figure 12 shows the fracture toughness results from the previous section as a function of molar mass. These show that at molar masses higher than 18 kg/mol, the fracture toughness remains constant, while at molar masses lower than 18 kg/mol, it decreases linearly. Back in 1988, Greco and Ragosta [25] observed similar results on neat polypropylene specimens and identified the molar mass transition as the critical molar mass. The latter usually defines a change from ductile to brittle behaviour, which was observed here, as shown in Figure 8. A critical molar mass can therefore be identified as M'_c=18 kg/mol. This value lies in the same range as those identified for other semi crystalline polymers with a glassy amorphous phase such as PET [24] and PA11 [20]. This confirms that fibres do not play any role in the degradation. As stated earlier, carbon fibres are rather insensitive at these temperatures. Additionally, the molar mass has proved to be a very interesting aging marker for neat polymers. Results from this study show that this is also true for long fibre reinforced composites. However, it would be of particular interest to investigate whether this behaviour is also valid under fatigue loadings.

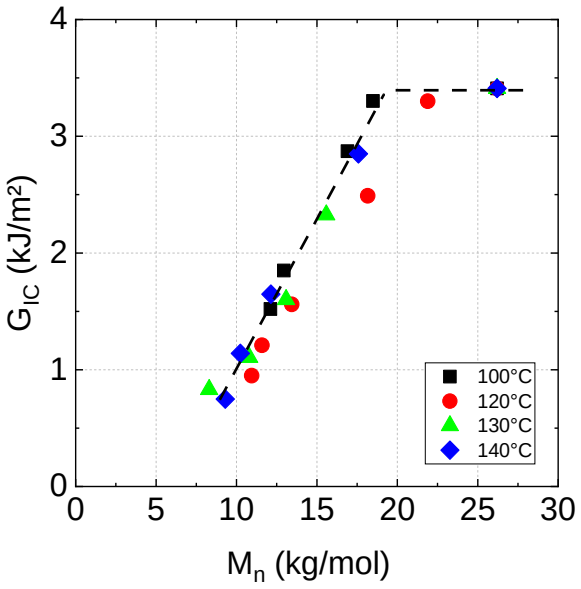

Figure 12: Fracture toughness as a function of molar mass (dashed line plotted for ease of reading)

4.2. Validity of the Arrhenius approach

The results presented above have shown that wet aging has a large effect on both the mechanical and physico-chemical properties of C/PA6 specimens. To translate the results from accelerated aging to service temperature (ambient temperature), an Arrhenius approach can be used [38,39]. The use of such an approach implies that the degradation observed is only activated by temperature and is due to only one process. The translation can be done through the adjustment of an accelerating factor a_t, defined in Equation 5.

$$a_T = exp\left[\frac{E_a}{R}\right].\left(\frac{1}{T_{ref}} - \frac{1}{T}\right) \quad \text{Eq.5}$$

Where E_a is the activation energy in J/mol, R the gas constant in $J.mol^{-1}.K^{-1}$ and T the temperature in K. The accelerating factor a_t is then used to shift the data from 140, 130 and 100°C onto the 120°C data, used here as a reference. This allows us to propose a master curve, Figure 13.

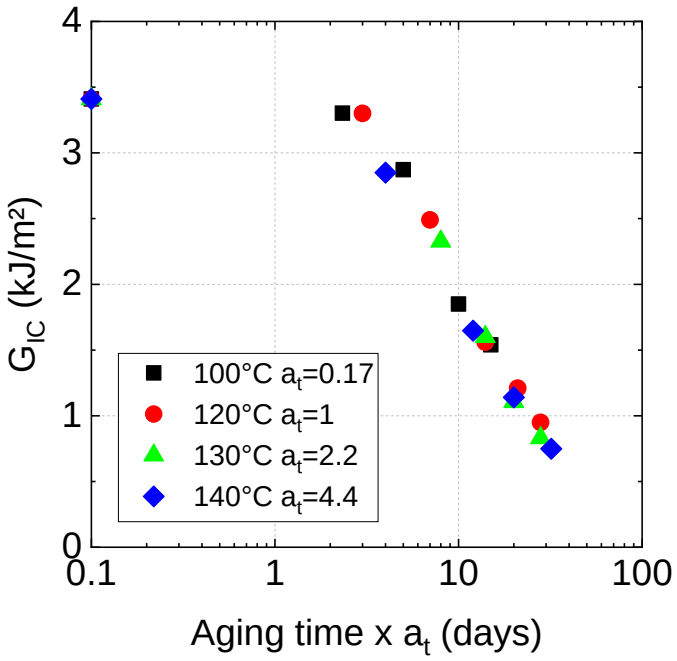

Figure 13: Master curve obtained from accelerated aging for the fracture toughness

The activation energy E_a can be obtained by plotting the accelerating factors as a function of 1000/RT, which allows the determination of the activation energy associated with fracture toughness changes. Such an approach can also be used for other parameters such as the molar mass, mass loss and crystallinity ratios, Figure 14. The associated activation energies are given in Table 1.

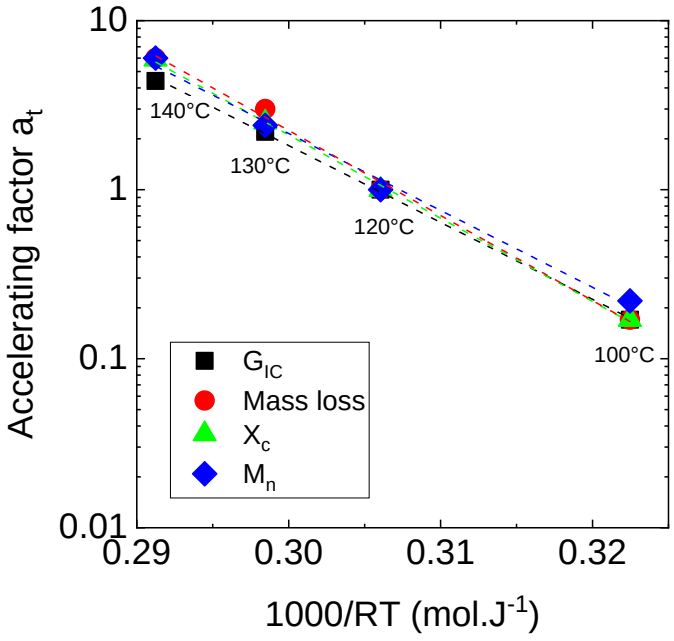

Figure 14: Arrhenius plots associated with each parameter

Table 1: Activation energies for the four parameters

Property	E_a (kJ/mol)	R^2
Fracture toughness	105	0.999
Molar mass	105	0.994
Crystallinity ratio	113	0.999
Mass loss	115	0.997

The activation energies found here all lie within a range from 100 to 110 kJ/mol. This suggest that the same mechanism is responsible for all the changes induced by aging, i.e. hydrolysis. It may be noted that comparable activation energies are found in the literature for pure hydrolysis. Deshoulles et al [30] obtained an activation energy of 106 kJ/mol for the mass loss on neat polyamide 6 and Bernstein et al [40] an activation energy of 102 kJ/mol on neat polyamide 66. This somewhat confirms that the carbon fibres do not play a significant role in the degradation. Additionally, in Deshoulles and Bernstein's work, it is also worth noting that their lowest aging temperature was 80°C. In both cases, after aging durations between 500 to 1000 days, they observed no decrease in the mechanical properties. This confirms that the degradation of both PA6 and PA6.6 is slow in pure hydrolysis conditions.

From these results, the accelerating factor associated with a temperature of 25°C is determined from extrapolation of Figure 14. This accelerating factor can then be used to extrapolate the data from fracture toughness at 120°C to 25°C, Figure 15. It may be noted that when the PA6 matrix is fully saturated with water, the glass transition decreases down to negative values [16]. Therefore, upon aging from 140°C down to 25°C, the material does not go through any phase transition. So the activation energy is assumed constant over this temperature range.

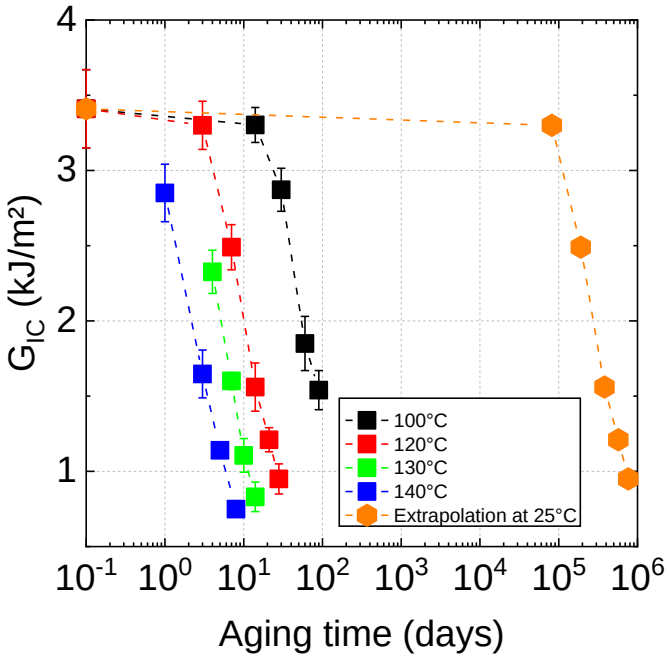

Figure 15: Extrapolation at 25°C

Using the extrapolation from Figure 14, it would take about 2000 years at 25°C to reach a fracture toughness value of 1 kJ/m², i.e. that of a good carbon/epoxy composite [3]. However, the extrapolation must be considered with caution, as it is only valid here for a material subjected to pure hydrolysis, i.e. without oxygen. Extrapolation was also performed at 80°C and 60°C to highlight that hydrolysis is indeed a slow process. It is fairly difficult to obtain highly degraded specimens at these lower temperatures, which justifies the chosen aging temperatures within this study. Indeed, it takes about 1000 days (~3 years) at 80°C and 8000 days (~20 years) at 60°C to reach a fracture toughness of 1 kJ/m². Nonetheless, this clearly demonstrates the excellent long-term behaviour of C/PA6 thermoplastic composites with respect to fracture toughness.

5. Conclusion

In this paper, the aging behaviour of carbon/polyamide 6 (C/PA6) composites subjected to pure hydrolysis was investigated by aging at different temperatures, ranging from 100 to 140°C. The changes in microstructure were assessed through physicochemical characterizations (crystallinity ratio, molar mass) and changes in mechanical properties were followed through mode I quasi-static crack growth tests. The results show that upon hydrolysis, the mode I fracture toughness decrease is related to the molar mass and that a ductile/brittle transition occurs at a critical molar mass value of 18 kg/mol. This was confirmed by the observation of fracture surfaces after failure. Finally, the results from accelerated aging were used to translate these high temperatures to realistic temperatures, i.e. ambient temperatures. Such an extrapolation has shown that pure hydrolysis in these C/PA6 laminates is a slow process. Indeed, upon aging in water without oxygen, it would take more than 2000 years for the mode I interlaminar fracture toughness of the C/PA6 laminate to drop from 3.4 kJ/m² down to 1 kJ/m². Future work will first focus on the assessment of the loss in fracture toughness upon hydrolytic aging under fatigue loadings. Moreover, this work is part of a project focused on the repair of thermoplastic composites after use in the marine environment, so the specimens tested here will be repaired. Their properties will then be compared to those obtained in this work before repair.

Acknowledgments

The authors would like to thank the scientific direction of Ifremer for the funding of the REPACOMP project.

References

[1] Cantwell, W. J., & Morton, J. (1991). The impact resistance of composite materials—a review. *Composites*, *22*(5), 347-362.

[2] Wong, K. J., Yousif, B. F., Low, K. O., Ng, Y., & Tan, S. L. (2010). Effects of fillers on the fracture behaviour of particulate polyester composites. *The Journal of Strain Analysis for Engineering Design*, *45*(1), 67-78.

[3] Sela, N., & Ishai, O. (1989). Interlaminar fracture toughness and toughening of laminated composite materials: a review. *Composites*, 20(5), 423-435

[4] Davies, P., & Rajapakse, Y. D. (Eds.). (2014). *Durability of composites in a marine environment* (Vol. 208). Dordrecht: Springer.

[5] Alam, P., Robert, C., & Brádaigh, C. M. Ó. (2018). Tidal turbine blade composites-A review on the effects of hygrothermal aging on the properties of CFRP. *Composites Part B: Engineering*, *149*, 248-259.

[6] Siriruk, A., & Penumadu, D. (2014). Degradation in fatigue behavior of carbon fiber–vinyl ester based composites due to sea environment. *Composites Part B: Engineering*, *61*, 94-98.

[7] Gagani, A. I., Krauklis, A. E., Sæter, E., Vedvik, N. P., & Echtermeyer, A. T. (2019). A novel method for testing and determining ILSS for marine and offshore composites. *Composite Structures*, *220*, 431-440.

[8] Marom, G. (1989). Environmental effects on fracture mechanical properties of polymer composites. In *Composite Materials Series* (Vol. 6, pp. 397-424). Elsevier.

[9] Le Guen-Geffroy A., Davies, P., Le Gac, P. Y., & Habert, B. (2020, December). Influence of Seawater Ageing on Fracture of Carbon Fiber Reinforced Epoxy Composites for Ocean Engineering. In *Oceans* (Vol. 1, No. 4, pp. 198-214). Multidisciplinary Digital Publishing Institute.

[10] Ochoa O, "Composite riser experience and design guidance," OTRC Final Project Report, 2006

[11] Salama M., Stjern G., Shorbaug T., Spencer B., and Echtermeyer A. T., "The First Offshore Field Installation for a Composite Riser Joint," presented at the Offshore Technology Conference, Houston, USA, 2002

[12] Arhant, M., & Davies, P. (2019). Thermoplastic matrix composites for marine applications. *Marine Composites; Woodhead Publishing: Cambridge, UK*, 31-53.

[13] Liu, H., Wang, J., Jiang, P., & Yan, F. (2018). Accelerated degradation of polyetheretherketone and its composites in the deep sea. *Royal Society open science*, *5*(4), 171775.

[14] Selzer, R., & Friedrich, K. (1995). Influence of water up-take on interlaminar fracture properties of carbon fibre-reinforced polymer composites. *Journal of materials science*, *30*(2), 334-338.

[15] Davies, P., & Arhant, M. (2019). Fatigue behaviour of acrylic matrix composites: influence of seawater. *Applied Composite Materials*, *26*(2), 507-518.

[16] Arhant, M., Le Gac, P. Y., Le Gall, M., Burtin, C., Briançon, C., & Davies, P. (2016). Effect of sea water and humidity on the tensile and compressive properties of carbon-polyamide 6 laminates. *Composites Part A: Applied Science and Manufacturing*, *91*, 250-261.

[17] Hoa, S. V., Lin, S., & Chen, J. R. (1992). Hygrothermal effect on Mode II interlaminar fracture toughness of a carbon/polyphenylene sulfide laminate. *Journal of reinforced plastics and composites*, *11*(1), 3-31.

[18] Davies, P., Pomies, F., & Carlsson, L. A. (1996). Influence of water absorption on transverse tensile properties and shear fracture toughness of glass/polypropylene. *Journal of composite materials*, *30*(9), 1004-1019.

[19] Zenasni, R., Bachir, A. S., Vinã, I., Arguelles, A., & Viña, J. (2006). Effect of hygrothermomechanical aging on the interlaminar fracture behavior of woven fabric fiber/PEI composite materials. *Journal of Thermoplastic Composite Materials*, *19*(4), 385-398.

[20] Jacques, B., Werth, M., Merdas, I., Thominette, F., & Verdu, J. (2002). Hydrolytic ageing of polyamide 11. 1. Hydrolysis kinetics in water. *Polymer*, *43*(24), 6439-6447.

[21] Fayolle, B., Audouin, L., & Verdu, J. (2000). Oxidation induced embrittlement in polypropylene—a tensile testing study. *Polymer Degradation and Stability*, *70*(3), 333-340.

[22] Okamba-Diogo, O., Richaud, E., Verdu, J., Fernagut, F., Guilment, J., & Fayolle, B. (2016). Investigation of polyamide 11 embrittlement during oxidative degradation. *Polymer*, *82*, 49-56.

[23] Fayolle, B., Audouin, L., & Verdu, J. (2003). Radiation induced embrittlement of PTFE. *Polymer*, *44*(9), 2773-2780.

[24] Arhant, M., Le Gall, M., Le Gac, P. Y., & Davies, P. (2019). Impact of hydrolytic degradation on mechanical properties of PET-Towards an understanding of microplastics formation. *Polymer degradation and stability*, *161*, 175-182.

[25] Greco, R., & Ragosta, G. (1988). Isotactic polypropylenes of different molecular characteristics: influence of crystallization conditions and annealing on the fracture behaviour. *Journal of materials science*, *23*(11), 4171-4180.

[26] Bardin, A., Le Gac, P. Y., Cérantola, S., Simon, G., Bindi, H., & Fayolle, B. (2019). Hydrolytic kinetic model predicting embrittlement in thermoplastic elastomers. *Polymer Degradation and Stability*, 109002

[27] Le Gac, P. Y., & Fayolle, B. (2018). Impact of fillers (short glass fibers and rubber) on the hydrolysis-induced embrittlement of polyamide 6.6. *Composites Part B: Engineering*, *153*, 256-263.

[28] Pegoretti, A., & Penati, A. (2004). Recycled poly (ethylene terephthalate) and its short glass fibres composites: effects of hygrothermal aging on the thermo-mechanical behaviour. *Polymer*, *45*(23), 7995-8004.

[29] ASTM D5528, (2007). *Standard test method for mode I interlaminar fracture toughness of unidirectional fiber-reinforced polymer matrix composites*. ASTM International

[30] Deshoulles, Q., Le Gall, M., Dreanno, C., Arhant, M., Priour, D., & Le Gac, P. Y. (2021). Modelling pure polyamide 6 hydrolysis: Influence of water content in the amorphous phase. *Polymer Degradation and Stability*, *183*, 109435.

[31] Mark, J. E. (Ed.). (2009). *Polymer data handbook*. Oxford University Press.

[32] Laun, S., Pasch, H., Longiéras, N., & Degoulet, C. (2008). Molar mass analysis of polyamides-11 and-12 by size exclusion chromatography in HFiP. *Polymer*, *49*(21), 4502-4509.

[33] Pemberton, R., Summerscales, J., & Graham-Jones, J. (Eds.). (2018). *Marine composites: design and performance*. Woodhead Publishing.

[34] Arhant, M., Le Gac, P. Y., Le Gall, M., Burtin, C., Briançon, C., & Davies, P. (2016). Modelling the non Fickian water absorption in polyamide 6. *Polymer Degradation and Stability*, *133*, 404-412.

[35] Serpe, G., Chaupart, N., & Verdu, J. (1997). Ageing of polyamide 11 in acid solutions. *Polymer*, *38*(8), 1911-1917.

[36] Rabello, M. S., & White, J. R. (1997). Crystallization and melting behaviour of photodegraded polypropylene I. Chemi-crystallization. *Polymer*, *38*(26), 6379-6387.

[37] Avella, M., Dell'Erba, R., Martuscelli, E., & Ragosta, G. (1993). Influence of molecular mass, thermal treatment and nucleating agent on structure and fracture toughness of isotactic polypropylene. *Polymer*, *34*(14), 2951-2960.

[38] Le Saux, V., Le Gac, P. Y., Marco, Y., & Calloch, S. (2014). Limits in the validity of Arrhenius predictions for field ageing of a silica filled polychloroprene in a marine environment. *Polymer Degradation and Stability*, *99*, 254-261.

[39] Ishisaka, A. A., & Kawagoe, M. (2004). Examination of the time–water content superposition on the dynamic viscoelasticity of moistened polyamide 6 and epoxy. *Journal of Applied Polymer Science*, *93*(2), 560-567.

[40] Bernstein, R., Derzon, D. K., & Gillen, K. T. (2005). Nylon 6.6 accelerated aging studies: thermal–oxidative degradation and its interaction with hydrolysis. *Polymer degradation and stability*, *88*(3), 480-488.